J Therm Anal Calorim (2015) 119:471–485
DOI 10.1007/s10973-014-3976-z

Effect of operating conditions on wax deposition in a laboratory flow loop characterized with DSC technique

Wenda Wang · Qiyu Huang · Changhui Wang · Si Li · Wenxing Qu · Jiadi Zhao · Manqiu He

Received: 4 December 2013 / Accepted: 16 June 2014 / Published online: 7 October 2014

Abstract In this paper, an experimental study about the influence of operating conditions in a laboratory flow loop on wax deposition phenomena by using DSC technique is presented. The operating conditions studied were oil temperature, wall temperature, temperature difference (between the bulk and the ambient), and flow velocity. Results were obtained and explained in terms of deposition rate and wax deposit composition (DSC curve shape). So that higher deposition rate was obtained for the following cases: oil temperature increasing, wall temperature decreasing, and at lower flow velocities. On the other hand, a wax deposit with heavier hydrocarbons was obtained when all the operating conditions evaluated were increased. These results will facilitate a better understanding of the physic of the wax deposition. Also, it will help in developing "hardness" model of the wax deposit, and thus provide a solid bearing on the pigging operation in petroleum industry.

Keywords Wax deposition · Operating conditions · DSC · Flow loop · Deposit composition · Hardness · Pigging

Introduction

Crude oil is a mixture of a diverse group of paraffins, aromatics, naphthenes, resins, asphaltenes, etc. Among these groups of hydrocarbons, heavy paraffinic hydrocarbons (waxes) can cause wax deposition on the pipeline wall when pipeline is subjected to a low environment temperature especially for deep sea [1]. It is encountered frequently during petroleum production and transportation. The temperature below which paraffin molecules start precipitating as wax crystals is referred to as the wax appearance temperature (WAT) or cloud point temperature [2]. When the temperature is lower than the WAT, solidification from paraffin crystals will preferentially occur on the cold pipe wall, then leading to deposition along with the oil trapped in the deposits. The wax deposition poses a very undesirable effect on pipeline with the increasing pump energy consumption and decreasing flow rate. In addition, precipitation of waxes significantly increases the crude viscosity and results in a poor flow ability of the crude changing from Newtonian to non-Newtonian behavior [3]. The crude begins to show non-Newtonian flow behavior at a certain temperature called the abnormal point [4], which is only a few degree Celsius below the WAT. Upon further cooling, more and more wax crystals precipitate from the oil and crystallize and in turn interlock to form a wax crystal lattice. This may lead to the oil gelling problem and even the blockage of the pipeline. Hence, wax deposition has always been a focus in flow assurance.

Some classic mechanisms for wax deposition, involving molecular diffusion in terms of liquid waxes, shear dispersion with respect to the transport of solid waxes in the particulate state, Brownian diffusion, and gravitational settling, were early proposed to explain this particular phenomenon [5–17]. Molecular diffusion is considered as the dominant mechanism responsible for the wax deposition in most cases and it is used in most prediction models of wax deposition, whereas the effects of gravity settling and Brownian diffusion have been ruled out [15–20].

W. Wang · Q. Huang (✉) · C. Wang · S. Li · W. Qu · J. Zhao · M. He
National Engineering Laboratory for Pipeline Safety/Beijing Key Laboratory of Urban Oil and Gas Distribution Technology, China University of Petroleum, Beijing 102249, People's Republic of China
e-mail: ppd@cup.edu.cn

However, the effect of shear dispersion on wax deposition was always controversial. But it has never been dismissed as a wax deposition mechanism. Later, Singh et al. [1, 21] proposed the mechanism of wax aging, which can be interpreted as counter-diffusion of different hydrocarbons from the deposit layer, thereby increasing its wax content and making the wax removal process more difficult. In addition, shear reduction for wax deposition including sloughing effect plays a significant role in the overall accumulation of waxes. More importantly, the removal of wax deposit by shear forces becomes more significant while the flow regime changes from laminar to turbulent flow. The sloughing effect also alters the morphology and nature of the deposit [18, 19, 22–25]. At the same time, the heat and mass transfer mechanism behind the wax deposition was well clarified [1, 12–36]. On this basis, various prediction models have been developed to describe the wax deposition in the last decades [6, 7, 9, 12, 16, 21–49]. However, modeling wax deposition still has scope for advancement [50].

Depending on the chemical composition of the crude oil and the operating conditions, wax deposition can occur in many climates [51]. Accordingly, the resultant wax deposits from different operating conditions also exhibit various features. For wax deposit on pipe wall, oil trapped in the wax matrix can represent up to 90 % of the deposit by volume [6]. The characteristics of wax deposit are predominantly influenced by its oil content and carbon number distribution for waxes, which are affected by a variety of operating factors. Thus an in-depth description of the wax deposition process will facilitate a better understanding of these factors.

Venkatesan et al. [24, 52] concluded that the yield stress of wax deposits is a strong function of the thermal and shear conditions under which the deposit experienced. Hoffmann et al. [19] deduced from wax deposition flow loop experiments that wax content in the deposits increases with the increasing wall temperature, flow rate, and experimental runtime. Huang et al. [53] reported the effect of operating temperature on wax deposition thickness by introducing the mass driving force. But Bidmus and Mehrotra [54] pointed out that Huang et al. [53] neither distinguished between the "cold flow" [55] and "hot flow" conditions [33] nor interpreted the actual role of thermal driving force in affecting the wax deposition correctly, instead attributed erroneously an incorrect generalization to them. Valinejad and Solaimany Nazar [56] evaluated the contribution of important operating factors such as inlet crude oil temperature, temperature difference between the oil and pipe wall, flow rate of the crude oil, wax content, and time on the amount of deposited wax statistically using the Taguchi experimental design approach. In addition, it was found that the aging process responsible for oil/wax content in the wax deposit is temperature-dependent [1, 21, 27, 29, 31, 57].

Table 1 Componential analysis result based on SARA method

Component	Saturates	Aromatics	Resin	Asphaltene
mass %	73.1	15.6	8.3	3.0

Table 2 Physical properties of the oil sample

Density at 20 °C/ kg m^{-3}	Gel point/°C	Abnormal point/°C	Wax appearance point/°C	Wax content/ mass %
850	6	17	20	7.1

However, despite significant progress has been made in this field in the past few decades, a full understanding of wax deposition characteristics under different operating conditions is still lacking. Pigging operations as the most effective maintenance tools are routinely used to remedy the wax deposition problems. This additionally requires an in-depth understanding for wax deposition process. Therefore, in this work, a systematic investigation of wax deposition characteristics under different operating conditions was conducted in a small-scale flow loop apparatus by using DSC technique. All the experiments were performed at wall shear stresses and operating temperatures typical of oil pipeline to simulate the wax deposition in the real pipeline. In addition to the growth of the deposit thickness, the composition of the wax deposit was specially investigated by a special designed method. Experimental results provide comprehensive insights into the wax deposit characteristics, laying a solid basis for the optimal pigging design in crude oil pipelines.

Experimental

Waxy crude oil sample

The experimental oil was sampled from a long distance pipeline. It was previously dehydrated in field by operator with water cut less than 0.5 mass %. For the waxy oil sample, the componential description and viscosity-temperature chart are shown in Table 1 and Fig. 1, respectively. Both the WAT and wax content of the oil sample were determined by DSC at a cooling rate of 5 °C min^{-1}. The DSC curve for the investigated oil sample is shown in Fig. 2. Table 2 gives a summary of some important physical properties of the oil sample. DSC and Cross Polar Microscopy are preferred methods to determine the WAT. However, WAT can also be recorded as the temperature of the deviation of the Arrhenius law as reported in literature

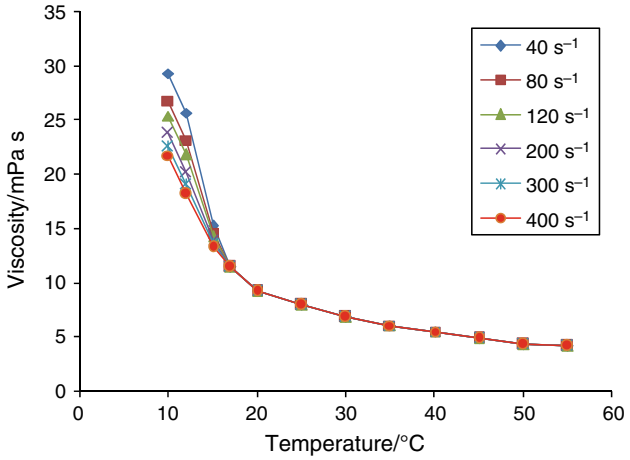

Fig. 1 Viscosity versus temperature at different shear rates

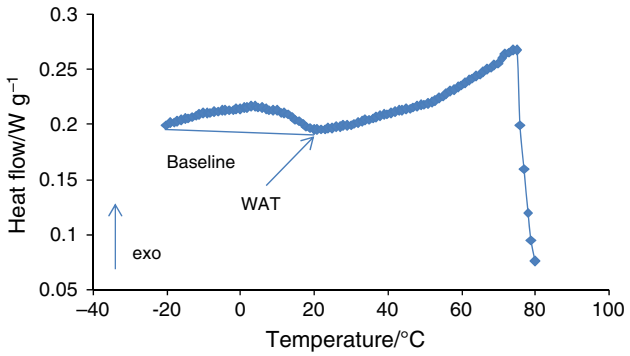

Fig. 2 Thermal spectra curve of the investigated oil sample during cooling

[58, 59]. It is clear that there is a good agreement in WAT value for two different determination methods, as presented by Figs. 1 and 2.

Wax deposition flow loop apparatus

A laboratory flow loop was used to perform the wax deposition tests, as shown schematically in Fig. 3. This experimental apparatus can operate under tightly controlled wall shear rates and temperature gradient conditions that reflect actual operating conditions in pipelines. In addition, the test section in the flow loop is removable (demountable), which allows to visually inspect the wax deposit, to determine the deposit mass by weighing, and to retrieve wax deposit sample for measurements of its physical properties during any stages of the wax deposition process.

The experimental apparatus consists of a stirred oil tank, a buffer tank, two delivery pumps, a pipe system, a circulating water system, and a data acquisition system. The experimental pipe system consists of the reference and test sections, which are made of two stainless-steel pipes of $\varphi 14 \times 1$ mm, with a length of 1.5 m. They are encapsulated by a water jacket of $\varphi 30 \times 1$ mm and packaged with an insulating layer. Recirculation water through the annulus supplied by water bath is used to control the wall temperature of the test and reference sections, with a maximum 0.2 °C deviation from the desired temperature throughout the experiment. The rest pipe sections between the test and reference sections are well insulated and electrically heat treated to prevent the accumulation of wax deposit. The tank volume is 20 L, and it is large enough to avoid the wax depletion. This oil reservoir feeding the oil into the flow loop is immersed in a hot water bath to heat the oil to the specified testing temperature. In addition, a matched stirring paddle may be employed to agitate the oil sample confined in the oil tank to obtain a uniform temperature distribution. Screw and peristaltic pumps are used to drive the flow of oil through the flow loop, and the flow rate can be varied by adjusting the electric motor speed. A liquid mass flow-meter with a range 0–600 kg h^{-1} and accuracy 0.25 % is used to monitor the mass flow rate. Specially, a peristaltic pump is equipped to avoid the crude sample changing during experiments due to the shear effect. The buffer tank next to the peristaltic pump can effectively eliminate the resulting fluctuation from the flow and shear. A bypass is installed on both ends of mass flow-meter to facilitate calibration for the flow rate. Thermocouples with a maximum error of 0.2 °C are installed in the oil tank, in the outlet of the pump, in the inlet and outlet of the test section, in its jacket, in the reference section, and in the outlet of its jacket to monitor the temperatures. Two differential pressure indicators, with a maximum range of 186 kPa and accuracy of 0.1 %, are placed over the test and reference sections, which can be used to measure the pressure drop over the test and reference sections so as to calculate the thickness of wax deposit. In addition, a data acquisition system can continuously record the flow rates, wall temperatures, and inlet temperatures of the fluid along with differential pressure readings in the test and reference sections. The calculated wax deposition thickness is displayed on the computer screen in real time to monitor the wax deposition process. Other details of this flow loop can be found in the literature [47].

DSC

At present, DSC technique is widely used to quantify the wax precipitation by virtue of its simplicity and fast response in petroleum industry [60–68]. In this work, both the deposited waxes and crude oil samples were performed thermal analyses using a computer-controlled TA2000/MDSC2910 DSC apparatus. The DSC has a 0.1 μW heat flux accuracy and 0.1 °C temperature-controlled accuracy.

During a DSC analysis, the apparatus was continually flushed with N_2. The sample is first loaded into the aluminum pan within the apparatus and heated to 80 °C, held

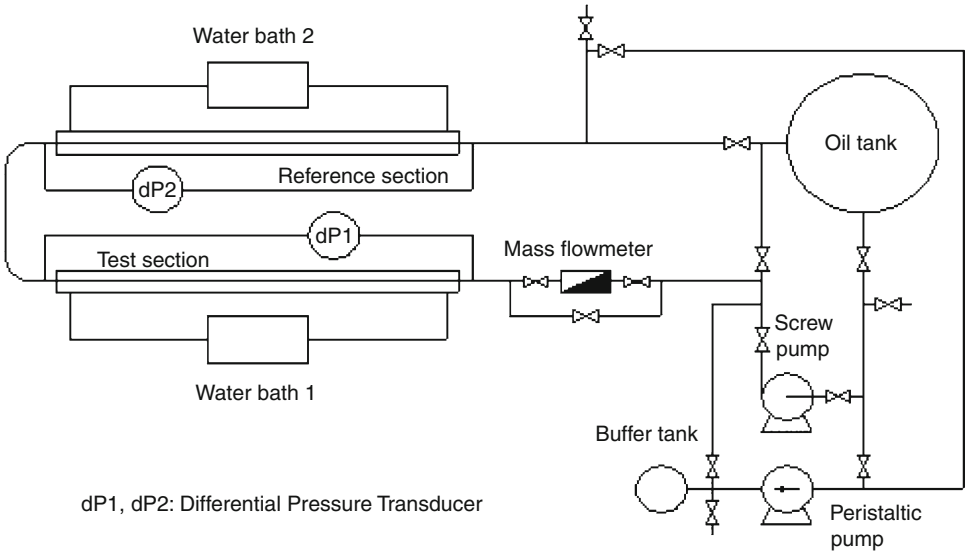

Fig. 3 Schematic diagram of the experimental apparatus for wax deposition

at this temperature for one minute and then cooled from 80 to −30 °C at a cooling rate of 5 °C min^{-1}. In the programed cooling range, the temperature of the test sample tends to be higher than the reference sample because of the release of latent heat during wax crystallization. In this process, the temperature difference ΔT turns from zero to non-zero. In order to keep ΔT at zero and keep the test and reference samples the same at the programmed temperature, the DSC automatically supplies different heat flows for the test and reference samples, and draws a thermal spectra to show the relationship between the heat influx and temperature. In the thermal spectra, the heat influx curve of the test sample deviates from the reference baseline to form a heat flow peak, because of the release of produced heat in the process of phase change involved. With the wax precipitation decreasing, both the phase-change-produced heat and temperature difference drop accordingly until the two curves superpose.

The temperature point in the cooling curve that starts to deviate from the baseline is called the wax appearance temperature (WAT). And the curve peak corresponds to the so-called wax peak temperature. The integral area between the heat flow curve and the baseline from WAT to −20 °C was used to calculate the average wax crystallization latent heat. With the average heat of wax crystallization, the wax content of the sample can be obtained. In addition, by measuring the average wax crystallization latent heat during phase transition and assuming the constant enthalpy of crystallization, the concentration of precipitated wax as a function of temperature or the wax precipitation curve (WPC) can be obtained. The fundamental of this method is established on the fact that the heat released by the test sample during cooling is proportional to the amount of precipitated wax [47, 69, 70].

Viscosity and gel point measurement of the crude oil

The viscosity profile was measured by the coaxial cylinder sensor system MVDIN of HAAKE VT 550 viscometer under the guidance of the Chinese Standard Petroleum Test Method SY/T 0520-2008. The water bath of HAAKE C25P was used for temperature control with an accuracy of 0.1 °C. The sample was transferred to the coaxial cylinder system preheated at the same temperature as that of the sample, then cooled the sample to the test temperature at the cooling rate of 0.7–1.0 °C min^{-1}, and kept at that test temperature for 15–20 min before the test. Then, the test was started, and the viscosity characteristics under different shear rates were measured. All the tests were repeated three times for each experimental condition, and the repeatability was good.

The gel point was determined by the Chinese Standard Petroleum Test Method SY/T 0541-2009. As stipulated by the method, the sample was firstly transferred to the gel point tube preheated at the sampling temperature, and then cooled at a rate of 0.5–1.0 °C min^{-1}, and the flow ability was checked at an interval of 2 °C to determine whether the sample was gelled or not from 8 °C above the expected gel point. The gel point is defined as the highest temperature at which the movement of the sample surface by gravity in a test tube cannot be observed when the tube is held horizontally for 5 s. In this study, the measured gel point was finally obtained from three repeated tests for each experimental condition, and the reproducibility was good. For the repeatability of rheological measurements and uniformity of the sample, the experimental crude was heated to 55 °C and then sampled to measure the viscosity and gel point before starting every flow loop experiment run.

Deposit thickness determination

At present, there is no technique that enables direct and continuous measurement for the thickness of wax deposits during experiments. In addition to the traditional weighing method, other indirect measurements, such as the pressure-drop method, heat-transfer method, and liquid displacement-level detection (LD-LD) method, have been applied to determine the thickness of wax deposits [71–73]. The pressure-drop and heat-transfer methods are established based on the principle that wax deposition inside the pipe increases the frictional pressure drop and insulating effect. The pressure-drop method can be performed online without interrupting the experiment and it is the only method available that can record the development of the wax thickness over time. In the application of the heat-transfer method, the thermal conductivity of the wax deposits must be known in advance. However, it is highly dependent on the wax content. Since the wax content is changing with time (aging) [1, 21], there is no reliable way to determine the thermal conductivity of the wax deposits accurately. This becomes the major difficulty for applying the heat-transfer method. Additionally, measurements using the above two methods cannot reflect the non-uniform distribution of the wax deposit along the axial and circumferential direction. To overcome this limitation, an online measurement of the deposit thickness, the LD-LD method, based on the volumetric displacement method at the end of each test, has been developed. It enables the measurements of spatial distribution of the wax thickness, which is not captured by the traditional methods [73]. Due to the complexity involved, this method was not used in the current study. A promising laser technique to determine asymmetric distribution of the wax thickness was reported by Hoffmann et al. [19]. This laser-based optical method, inspired by Chakrabarti et al. [74], is also capable of detecting spatial variations of the wax deposits but only when the experiment is interrupted.

In this study, the weighing method was used to determine the deposit thickness throughout the experiments due to its reliability and laboratory limitation. At the end of the experiment, the deposits were collected from the test section in the flow loop to estimate the mass. Note that the remaining oil in the test section must have been completely drained for applying the weighing method. The measured deposit thickness is an average over the test section. Although the real circumferential and axial deposit thickness distributions cannot be exactly obtained by the weighing method, the average deposit thickness can also reflect the wax deposition characteristics under different operating conditions well.

Wax deposit composition analyses

In order to further investigate the deposit composition characteristics under different operating conditions, in this study, the test section tubing was removed from the flow loop after each experiment and then the deposit samples were collected for further DSC analyses. The percentage of groups of wax species present in total wax content during the crystallization of the deposits that would crystallize out at different cooling temperatures in terms of constant temperature interval of 5 °C was determined in detail by DSC analyses. By this way, another form of WPCs for the collected deposits was obtained. In this work, this method was used to pronounce the effect of operating conditions on the wax composition of deposits. In addition, WAT of the deposits was also investigated to extrapolate information about their wax composition.

Experimental design and procedure

It is well known that no deposition occurs when the wall temperature in the pipeline is always higher than the WAT. Hence, during the experiments, the wall temperature of the test section is maintained below both the WAT and oil temperature to induce wax to be deposited on the cold pipe wall. However, contrary to the test section, the wall temperature of the reference section is kept at the same temperature as that of the oil to prevent the wax deposition. Moreover, before the waxy oil sample enters the test section, it flows through an entry section with length over 1 m to allow the oil flow to be fully developed at the test section. All the tests are started after removing the molten deposits from the flow loop completely, and all the instruments including the mass flow rate meters are all pre-calibrated before starting each experimental run. Since the maximum achievable Reynolds number based on the cross-sectional averaged speed and inner diameter is $\sim$2,000, all the experiments were conducted in laminar flow.

In a typical flow loop run, the crude oil is first poured into the feeding tank and heated to the desired temperature for removing any thermal history, and then the crude oil is allowed to cool slowly to the experimental temperature. During this process, the crude sample is continuously stirred in the tank. The temperature in the water bath at the reference section is adjusted to the oil temperature, and the temperature in the water bath at the test section is maintained at the experimental pre-set temperature which is below the oil temperature. Oil is then pumped into the flow loop from the feeding tank through the test and reference sections, ultimately returned to the oil tank. When the wax deposition reaches certain level or time interval, oil flow will be stopped. Pressurized air is then used to clean up the

residual oil out of the flow loop from the oil draining hole. The air pressure is kept at a certain value so that it generates the same shear force on the wax layer as the oil flow does and thus the wax deposit layer does not change its characteristics. After that, the test section is demounted from the flow loop. Then the temperature of recirculation water flowing through the annulus between the water jacket and the text section is raised up to a high temperature by controlling the water bath until all the wax deposits in the pipe wall are completely molten. At last, the flowing molten deposits were collected in a weighing beaker for the weighing and DSC analysis.

Results and discussion

In this section, the average deposition rate was calculated from the deposit mass to compare the deposit formation under different operating conditions qualitatively. Also DSC analysis regarding WAT and WPC was performed for the deposit samples retrieved from the flow loop tubing after each experiment to interpret the wax composition of the deposit.

Effect of inlet oil temperature on deposition

Waxy crude oil flow will almost certainly be turbulent in the long distance pipelines due to the large diameters. Based on a turbulence correlation of the Darcy/Fanning friction factor with the Reynolds number on a smooth pipe, the shear rate of a Newtonian fluid in turbulent flow in a real pipeline can be calculated from Eq. (1) [75, 76].

$$\dot{\gamma}_w = 4.94 \times 10^{-3} \mathrm{Re}^{0.75} \frac{8V}{d} \quad (1)$$

where $\dot{\gamma}_w$ is the pipe wall shear rate in s^{-1}, *Re* the Reynolds number, *V* the oil flow velocity in m s^{-1}, and *d* is the inner pipe diameter in m.

Thus, the typical operating conditions at wall shear rates and, therefore, wall shear stresses for the target export line of $\phi 610 \times 8$ mm are determined by Eq. (1), as shown in Table 3. It is observed from Table 3 that the pipe wall shear stresses are approximately on the order of 1–6 Pa. This stress level falls into the range of applicable shear stresses (1–10 Pa) typically encountered in the export lines as reported by Tinsley [18]. In order to ensure the reliability of the flow loop simulations, the flow loop tubing wall shear rate (or shear stress) has to be tightly controlled to equal to that of the actual field pipeline as revealed above. So throughout the experiment involved in investigating the wax deposition characteristics under different thermal conditions, the experimental flow velocity in the flow loop is always maintained constant at 0.30 m s^{-1} (corresponds to a shear rate of 200 s^{-1}) based on the shear rate formula [Eq. (2)] for the laminar flow in the laboratory flow loop [75].

$$\dot{\gamma}_w = \frac{8V}{d}. \quad (2)$$

The inlet crude oil temperature is observed to be of secondary in importance among factors affecting wax deposition amount by Valinejad and Solaimany Nazar [56]. In order to investigate the effect of the inlet oil temperature on deposition, an oil sample with 7.1 mass % of wax dissolved entered the test section at different inlet oil temperatures, where the wall temperature of the test section tubing was maintained constant at different levels for 10, 15, and 17 °C, respectively. Fig. 4 shows the average deposition rate and the WAT of the deposit formed at different oil temperatures and constant wall temperatures (10, 15, and 17 °C). It is observed from Fig. 4 that as the oil temperature increases, the deposition rate for different operating wall temperature levels increases similarly with different steps. In the case that the wall temperature was kept constant at 10 °C, the deposition rate grows at a fast linear rate initially and then decreases to a slower rate until it reach the maximum after the ΔT exceeds 5 °C (oil temperature above 15 °C). It is emphasized that with a WAT of 20 °C for the investigated oil sample, the experiments were performed with constant wall temperature of 10 °C and oil temperatures between 12 and 20 °C—referred to as the "cold flow" conditions. This result is in agreement with the conclusion made by Bidmus and Mehrotra [33]. In contrast to this case, the deposition rate increases almost continuously but not sharply when the operating wall temperature is much higher (15 and 17 °C), and no sign of level off in the curve was observed. In short, the effect of the operating oil temperature in the lower wall temperature level (10 °C) is more significant than in the higher wall temperature levels (15 and 17 °C). Experimental results confirmed the fact that the increasing driving force for heat transfer, ΔT, always accelerates the wax deposition.

As reported previously by Huang [53] and Han [67], the precipitation characteristics of the dissolved wax in oil is closely related to the shape of the DSC curve of the tested oil sample, so the gradient of solubility with respect to temperature greatly affects the precipitation and thus the deposition. Hence, the DSC curve as shown in Fig. 2 can be used to explain the observed variation trends of the deposition rate in Fig. 4. It can be seen from Fig. 2 that the thermal spectra curve of the tested oil sample just starts to deviate from the baseline gently when the oil temperature decreases from 20 to 15 °C. This indicates the wax molecules start to precipitate out of the solution and a small amount of wax crystals appear in the solution in this

Table 3 Conditions for shear rate and shear stress regimes operated in the studied pipeline

Flow velocity/m s^{-1}	"Low" flow rate $G = 400 \times 10^4$/t a^{-1} 0.60	"Moderate" flow rate $G = 600 \times 10^4$/t a^{-1} 0.89	"High" flow rate $G = 1{,}000 \times 10^4$/t a^{-1} 1.48
Fluid viscosity $\mu = 10$ mPa s			
Wall shear rate/s^{-1}	91.6	182.8	445.1
Wall shear stress/Pa	0.92	1.83	4.45
Fluid viscosity $\mu = 20$ mPa s			
Wall shear rate/s^{-1}	54.5	108.7	264.6
Wall shear stress/Pa	1.09	2.17	5.29
Fluid viscosity $\mu = 30$ mPa s			
Wall shear rate/s^{-1}	40.2	80.2	195.1
Wall shear stress/Pa	1.21	2.41	5.85

The pipeline investigated in this work has a geometrical dimension of $\phi 610 \times 8$ mm

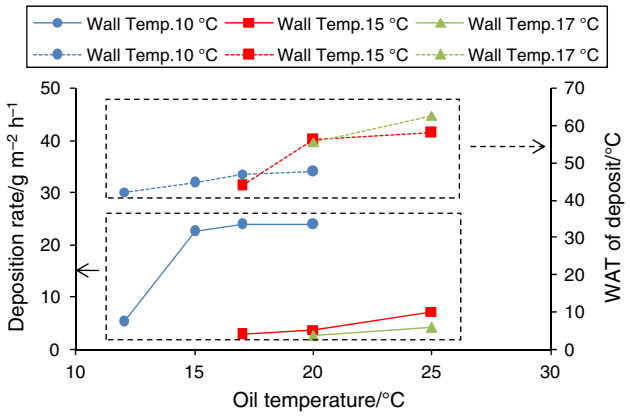

Fig. 4 Average deposition rate and WAT of the flow loop deposit as a function of oil temperature under constant wall temperature (10, 15, and 17 °C)

temperature range. The solubility factor of wax in oil becomes much higher, and the amount of the precipitated wax crystals in the solution begins to increase rapidly when the cooling temperature changes in the range of 10–15 °C, indicated by a steep rising in the DSC curve. Hence, it can be concluded that more wax crystals would precipitate near the pipe wall and then probably participate in the wax deposition process at lower operating wall temperature condition of 10 °C. In this case, the shear dispersion may be believed to be the principal mechanism responsible for the deposition process, instead ΔT as the driving force for molecular diffusion becomes a much weaker influential factor for wax deposition, and thereby, the deposition rate at the oil temperature above 15 °C for this lower wall temperature condition (10 °C) is almost the same (corresponds to the level section in Fig. 4). In comparison to the higher oil temperature condition (>15 °C), the precipitated waxes with lower carbon numbers are in the majority of the solution in the lower oil temperature condition of 12 °C (as will be explained below), although the concentrations of precipitated waxes in the solution are higher in such low oil temperature. Thus, the resulted wax deposit may incorporate more waxes with lower carbon numbers. However, the adhesive force of those lower carbon number waxes is much weaker, and part of them is easily eroded by the stronger fluid shear force induced by the lower oil temperature and thus higher viscosity (the sloughing/erosion effect), in which the adhesive failure between the waxes and the deposition substrate occurs. Hence, the deposition rate in lower oil temperatures is much lower.

For higher wall temperatures (15 and 17 °C), the corresponding operating oil temperature mainly ranges from 20 to 25 °C (WAT = 20 °C) as shown in Fig. 4, so essentially the waxes are all dissolved in the bulk flow. In this case, the molecular diffusion induced by the temperature gradient from the bulk toward the pipe wall is the predominant mechanism responsible for the wax deposition. Using the molecular diffusion equation [Eq. (3)], the dependence of wax deposition rate on oil temperature can be illustrated as follows. As the oil temperature increases, the temperature gradient $(\mathrm{d}T/\mathrm{d}r)$ and in turn the concentration gradient of dissolved wax in oil $(\mathrm{d}C_\mathrm{w}/\mathrm{d}r)$ increases. In addition, the higher temperature results in a lower viscosity of the crude, thus a higher diffusion coefficient (D_w) [see Eq. (4)]. As a result, the deposition rate increases with the increasing oil temperature for constant higher wall temperatures. This conclusion is consistent with the results reported by Lashkarbolooki et al. [72] and Creek et al. [77].

The molecular diffusion model is given by

$$W = \rho_\mathrm{w} D_\mathrm{w} \frac{\mathrm{d}C_\mathrm{w}}{\mathrm{d}r} = \rho_\mathrm{w} D_\mathrm{w} \frac{\mathrm{d}C_\mathrm{w}}{\mathrm{d}T} \frac{\mathrm{d}T}{\mathrm{d}r}, \tag{3}$$

where W is the wax deposition rate in kg m^{-2} s^{-1}, ρ_w the wax density in kg m^{-3}, D_w the diffusion coefficient of wax in oil in m^2 s^{-1}, $\frac{\mathrm{d}C_\mathrm{w}}{\mathrm{d}r}$ the radial concentration gradient of dissolved wax molecule in m^{-1}, $\frac{\mathrm{d}C_\mathrm{w}}{\mathrm{d}T}$ the change of

dissolved wax concentration with temperature, i.e., the gradient of the wax solubility curve of the crude, 10^{-3} °C^{-1}, and $\frac{dT}{dr}$ is the radical temperature gradient near the pipe wall in °C m^{-1}.

The diffusion coefficient of wax in oil (D_w) in Eq. (3) can be written as follows:

$$D_w = \frac{B}{\mu}, \tag{4}$$

where μ is the viscosity of the crude oil in Pa s, and B is the coefficient and approximately constant for a given oil sample [6].

The wax composition of the deposit sample collected in previously mentioned conditions was investigated in terms of the WAT and WPC at different temperature intervals by DSC after each experiment. The variation of the WAT of the deposit obtained from the above experimental conditions is additionally illustrated in Fig. 4. It can be seen that the WAT of the wax deposit increases with the increasing oil temperature for constant wall temperatures. This indicates that the deposit formed at a higher oil temperature may have a higher wax distribution. Fig. 5 shows a comparison of WPCs for the wax deposits retrieved from the above experiments at different oil temperatures and three constant wall temperatures (10, 15 and 17 °C). Note that each datum for the mass fraction of crystallized waxes in the total wax content within the deposits was calculated from released heat influx during cooling at every constant temperature range of 5 °C. In short, the Y-axis on these plots denotes an accumulated amount for wax crystallization by mass (mass %). And X-axis displays an average temperature for each temperature drop region during cooling. This criterion is adopted for all WPCs over this work. Comparing the WPCs of the deposits for all the cases shows that a significant wax peak is present in the curves. This peak in the WPCs represents the maximum accumulated groups of wax species in the deposit at the corresponding temperature ranges. The WPCs for the deposits clearly show the wax peak temperature shifted from the low temperature toward the high temperature. In addition, it is seen that the region occupied by the waxes precipitated in the higher temperatures is increasing considerably for the higher operating oil temperatures. This is to say that the wax species physically deposited changes toward a higher carbon number and, therefore, a higher molecular mass distribution for a higher operating oil temperature. Deposits containing a great quantity of high molecular mass waxes might be expected to offer greater resistance to pigging. Such behavior follows the trends of the WAT of the deposit shown in Fig. 4 for the same deposition test. All these results imply a higher operating oil temperature contributes to a wax deposit with heavier hydrocarbons.

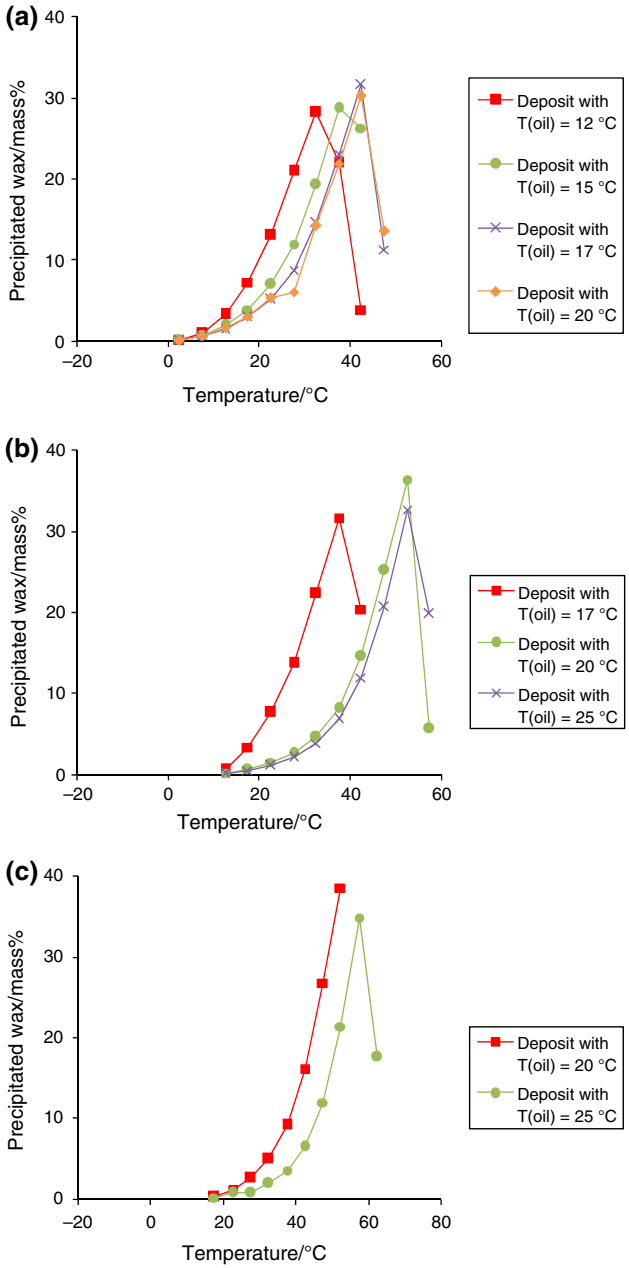

Fig. 5 Comparison of WPCs determined by DSC analysis for the flow loop wax deposits formed at different oil temperatures and constant wall temperatures: **a** 10, **b** 15, and **c** 17 °C

The reason why the wax composition in the deposits changes toward the heavier hydrocarbons for the higher operating oil temperatures is mainly related to the solubility limitation for the different wax species. For the relatively higher operating oil temperatures, the heavier hydrocarbons crystallized and precipitated first, and thereby preferentially deposited on the pipe wall whether or not the shear dispersion worked during the wax deposition. In addition, for the higher heat influx, the molecular diffusion is more prevalent, and the deposits laid down by

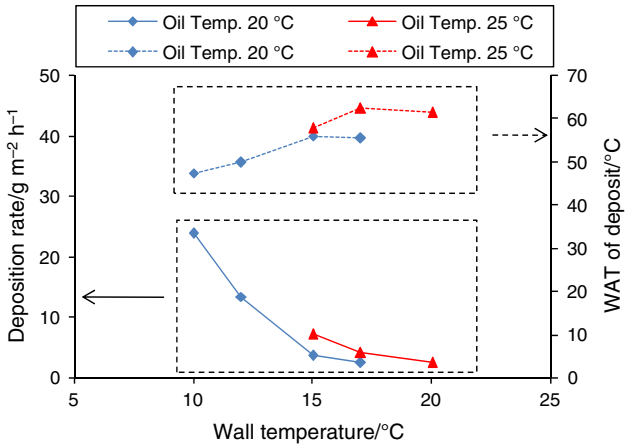

Fig. 6 Average deposition rate and WAT of the flow loop deposit for different wall temperatures and constant oil temperatures (20 and 25 °C)

molecular diffusion are consequently more compact in which less amount of oil was entrapped. The combination of these two effects leads to the wax composition in the deposits changing toward the heavier paraffins.

Effect of cold wall temperature on deposition

In a real application, the surrounding temperature of the pipeline changes with the variation in seasons, thus the wall temperature of the pipeline also varies concomitantly. Hence, in order to investigate the dependence of wax deposition on wall temperature, a series of experiments in the flow loop were performed at two constant inlet oil temperatures of 20 and 25 °C, respectively. The oil flow velocity is still held constant at 0.30 m s^{-1} as previously mentioned during the wax deposition experiments. The operating wall temperatures in the test section are tightly adjusted by water bath with recirculation water flowing in the annulus. Thus, the external wall temperature is always equal to the desired temperature throughout the experiments. Note that the wall temperature refers to the external wall surface temperature in this work. The experimental results are shown in Figs. 6 and 7, respectively.

Figure 6 shows that the deposition rate decreased as the wall temperature is increased for the two constant oil temperatures (20 and 25 °C). The main reason for this can also be interpreted by Eq. (3). In the designed experimental conditions (Oil temp. = 20 or 25 °C ≥ WAT = 20 °C), the molecular diffusion predominates the wax deposition. As the operating wall temperature is increased to approach the WAT, both the solubility factor of wax crystal near the pipe wall (dC_w/dT) as shown in Fig. 2 and the temperature gradient (dT/dr) decrease. It is concluded from Eq. (3) that therefore the deposition rate decreases correspondingly. In addition, as reported by Hoffmann et al. [19], the adhesion

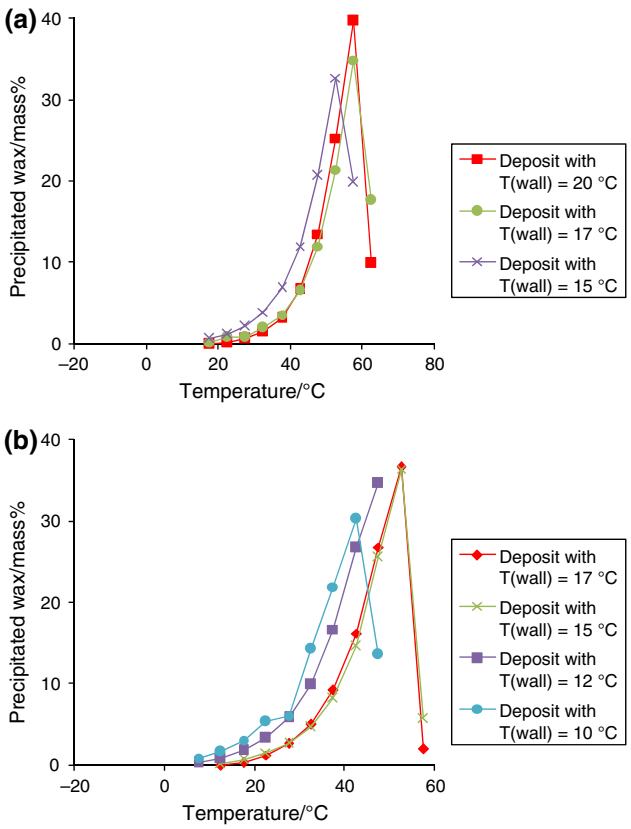

Fig. 7 Comparison of WPCs determined by DSC analysis for the flow loop wax deposits formed at different wall temperatures and constant oil temperatures: **a** 25 °C, **b** 20 °C

force between the deposit substrate and the pipe wall for the higher wall temperatures is so low that the deposited waxes are eroded from the pipe wall due to the sloughing effect. Thus, the deposition rate decreases considerably while the operating wall temperature is ramping up. Also, this result is in agreement with the conclusion made by Bidmus and Mehrotra [33].

Again, it is observed from Fig. 6 that in both two cases, the WAT of the deposit increases initially and then remains basically unchanged with the increasing wall temperature. The wax composition change in the deposit formed at varying operating wall temperatures and two constant oil temperatures (20 and 25 °C) is clearly reflected by Fig. 7. Similarly, both the wax peak temperature and the area under the wax peak in the WPCs shifted from the low temperature toward the high temperature with the increasing wall temperature. This result along with that of the WAT indicates that the fraction of heavier waxes (wax species with a higher carbon number or a higher molecular mass) deposited physically in the higher temperature region is increasing considerably for a higher wall temperature. For example, DSC analysis for the deposit formed at the operating oil temperature of 20 °C and wall

temperature of 17 °C shows that all the wax species crystallized at the temperatures above 15 °C, and wax components of 65.38 mass % crystallized at the temperatures above 45 °C during cooling. Whereas, the wax species for the deposit with operating wall temperature of 10 °C crystallized at the temperatures below 15 °C and above 45 °C accounted for 2.52 and 13.63 mass %, respectively. This result indicates that a higher operating wall temperature also leads to a wax deposit with heavier hydrocarbons. The results confirmed the experimental results of Singh et al. [21] and Hoffmann et al. [19].

As the operating wall temperature is increased, the temperature difference ΔT between the bulk flow and the pipe wall decreases. As a result, the molecular diffusion initiated by ΔT was weakened, and thus the dissolved hydrocarbon molecules transported by molecular diffusion toward the pipe wall were considerably decreased. Moreover, among the precipitated waxes in the vicinity of the pipe wall, wax crystals from heavier hydrocarbons are in the majority for the higher wall temperatures, because the lighter hydrocarbons cannot crystallize out of the crude at the relatively higher wall temperatures even if they substantially migrate to the pipe wall. Therefore, it is possible that such heavier hydrocarbons may participate in the deposition process preferentially. In other words, the deposit formed at the relatively higher wall temperatures is expected to be enriched in the heavier hydrocarbons.

Effect of constant ΔT on deposition

In this section, the effect of a constant temperature difference ΔT between the bulk and the ambient on the deposition characteristics has been studied. During the deposition process, the temperature difference ΔT was held constant, but the operating oil and wall temperatures were varied. In the first series of experiments, the oil flow velocity $V_{(oil)}$ was maintained constant at 0.30 m s^{-1}, but the oil and wall temperatures were changed synchronously to obtain a specified constant temperature difference ΔT (2 or 3 °C) starting with a initial oil temperature of 12 °C. In the second series of three experiments, the temperature difference ΔT between the oil and cooling medium was always 5 °C, and the oil flow velocity $V_{(oil)}$ was maintained the same constant value (0.30 m s^{-1}) as the previous conditions. And the oil temperature was increased for each experiment by 5 °C, starting at temperature of 15 °C for the first experiment in the second series.

Figure 8 shows deposition rate versus temperature for two different constant ΔT (2–3 and 5 °C). Hereof, the mean temperature represents an arithmetic average value calculated from the oil temperature and wall temperature. The oil flow velocity, $V_{(oil)}$, was maintained constant at 0.30 m s^{-1}. Several observations can be made from these

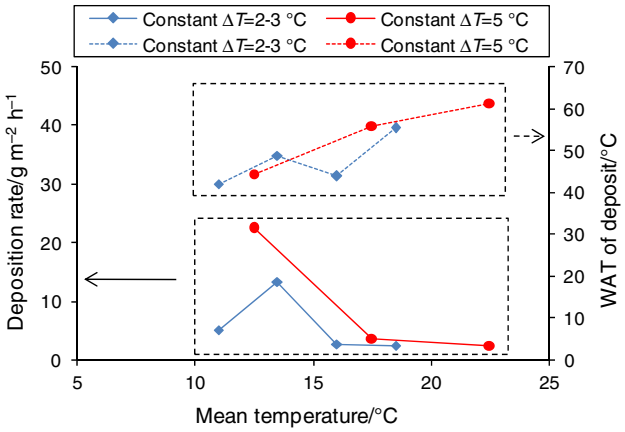

Fig. 8 Variation of average deposition rate and WAT of the flow loop deposit with mean temperature for two different constant heat-transfer driving forces (ΔT = 2–3, 5 °C)

results shown in Fig. 8. One is that wax deposition at an operating temperature difference ΔT of 2–3 °C was found to form a wax deposition peak somewhere in the interval between 11 and 15 °C. In fact, this wax peak corresponds to an operating condition in which the oil temperature and wall temperature is 15 and 12 °C, respectively. Another observation is that wax deposition at a constant temperature difference ΔT of 5 °C was found to be decreased with the increasing temperature. This discrepancy is contributed to the fact that the temperature difference ΔT reflects an overall behavior of the temperature or the interplay between the operating oil and wall temperatures. Also this confirms the conclusion on the other side that the effect of temperature difference ΔT between the bulk and the ambient is a more important parameter for wax deposition than that of the oil or ambient temperatures alone [56, 72].

The wax solubility curve has a significant influence on the wax deposition [53, 67], and thus the wax deposition characteristics at a constant temperature difference or temperature gradient condition can be well explained by the DSC curve. For the first series of experiments (ΔT = 2–3 °C), all the experiments were performed under "cold flow" conditions, in which the oil temperature was held below the WAT (20 °C) throughout the experiments. In this case, the shear dispersion with respect to solid wax particles is relatively prevalent comparing to the molecular diffusion regarding liquid wax molecules during the wax deposition process. It can be seen from Fig. 2 that the thermal spectra curve of the oil sample just starts to form peak until the temperature cools below 15 °C. Thus, only a small amount of wax molecules precipitate out of the solution in the relatively higher temperature range from 20 to 15 °C. This results in the fact that the wax deposition induced by shear dispersion is much lower for the above operating conditions. However, in the temperature range from 15 to 11 °C, the DSC curve starts to rapidly escalate.

Accordingly, the solubility factor of wax in oil becomes much higher, and a lot of precipitated wax particles in the bulk flow are present in such low temperatures. Thus, the shear dispersion allows the precipitated wax to participate in the deposition process actively. Hence, the wax deposition rate may be much higher in the temperature range of 11–15 °C. While the temperature continues to decrease to a lower value below 11 °C, the amount of the precipitated wax crystals is not increased any more. Instead, the lower operating oil temperature will lead to a wax deposit with the lower carbon number waxes, as has been explained in the previous section. It is easily removed by the shear due to the sloughing effect. Therefore, the deposition rate in the lower temperatures below 11 °C is also much lower. As a result, a wax peak is formed in the temperature range of 11–15 °C for the constant temperature difference condition (ΔT = 2–3 °C).

For an operating condition in which temperature difference ΔT was held constant at 5 °C, the greatest severe wax deposition is encountered while the oil temperature is specified at 15 °C (see Fig. 8). When the temperature increases, the wax deposition is weakened. This is closely associated with the fact that the growth tendency of the DSC curve (see Fig. 2) is much steep while the temperature drops below 15 °C. This result indicates that the amount of the precipitated wax crystals in the solution is a lot, and thus probably leads to much more severe wax deposition in the oil temperature of 15 °C under the control of the shear dispersion mechanism. When the oil temperature varied between 20 and 25 °C, the molecular diffusion regarding the migration of the dissolved wax molecules dominates the wax deposition. In this case, as the oil temperature increases, the wall temperature also increases due to the constant temperature difference condition. In other words, the higher oil temperature corresponds to a higher wall temperature. Thus, the amount of waxes precipitated in the vicinity of pipe wall is much less due to the higher operating temperatures. As a consequence, the concomitant wax deposition is much lower. In addition, Fig. 9 also shows the amount of precipitated wax from the oil sample at different temperatures. Note that in Fig. 9, the mass fraction of precipitated wax in the oil has been amplified tenfold to facilitate the comparison with that of the deposit. In fact, the mass fraction of precipitated wax in the oil is in a unit of mass ‰, whereas that of deposit is in a unit of mass %. Since the temperature difference has been constant for all the experiments, the wax deposition should follow the wax solubility curve and, therefore, the WPC. At comparable temperatures (Oil temp. = 20–25 °C), the two curves for deposition rate and WPC of the crude show a remarkable similarity, implying that the wax diffusion is indeed the major mechanism for wax deposition in this temperature range. In fact, the temperature region experienced the severe deposition

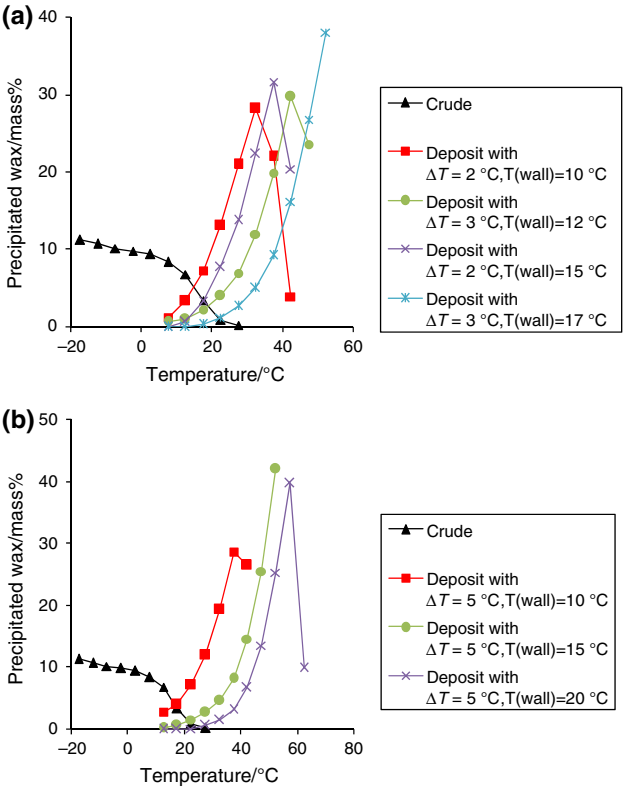

Fig. 9 Comparison of WPCs determined by DSC analysis for the flow loop wax deposits formed under different constant temperature differences ΔT between the bulk and the ambient: **a** 2–3 °C, **b** 5 °C

for constant ΔT = 2–3 and 5 °C, both falling into a certain temperature range (10–15 °C), in which the DSC curve escalate rapidly and much more waxes precipitate (Fig. 2).

In addition, the WAT of the deposit is also shown in Fig. 8. For all the cases, the WAT of the deposit increases with the increasing operating temperature. This indicates that the wax species physically deposited shifted toward the heavier hydrocarbons with a higher molecular mass while the operating temperature is increased at the constant ΔT. One exception is the operating condition for the oil temperature of 17 °C and wall temperature of 15 °C at the constant ΔT = 2–3 °C. This abnormality can be reasonably explained by the shorter running time compared to the other experiments. It can be also inferred that, based on the aging model [1, 21], if the experiment was run properly for a longer experimental time, the wax content in the deposit will definitely increase with time, and thus the WAT of the deposit will be high enough to confirm the trend of the curve well. Another interesting finding is that WATs of the deposit formed at two different temperature difference ΔT are approximately identical at the same operating conditions. This result is in line with the experimental results of Huang [69].

Figure 9 shows a comparison of WPCs for the wax deposits collected from the aforementioned experiments. Compared to the crude oil, the deposits in both cases show a significant wax peak from the high temperature to low temperature during crystallization. Comparison of the WPCs for the deposits in both cases shows that the main crystallization temperature domain in WPCs moved toward the higher temperatures for the higher operating temperatures and meanwhile shifted their center toward the higher temperatures. Specially, the WPC of deposit from the specified experiment in which the operating oil temperature and wall temperature were held constant at 17 and 15 °C, respectively, shows an inconformity for the graphic trend, as mentioned previously for the WAT of the deposit. This shift to a higher value of crystallization temperature again interprets the effect of operating temperature difference ΔT on wax composition of the deposits. The higher the operating temperatures are, the much heavier the hydrocarbons are included within the deposits. Similarly, the wax composition change for the deposit toward the heavier hydrocarbons may lead to an increasing hardness.

Effect of flow velocity on deposition

To understand the effect of flow velocity on the deposition, a separate series of deposition experiments were conducted in the laboratory flow loop at various flow velocities in the laminar regime. The oil sample with the temperature of 15 °C was flown through the flow loop at flow velocities 0.21, 0.30, 0.56, and 0.82 m s^{-1} corresponding to *Res* 107, 153, 286, and 418, respectively. The wall temperature of the tubing in the test section was kept constant at 10 °C during the experiments. Due to the varying flow velocities, the wall shear rate $\dot{\gamma}_w$, calculated by Eq. (2), varies from 140 to 547. The average deposition rate is smaller for a higher flow velocity, as demonstrated in Fig. 10.

As can be seen from Eqs. (5) and (6), the pipe wall temperature gradient increases with the increasing flow velocity (the increasing *Re*), and in turn so do the concentration gradient and the deposition rate in diffusion model [Eq. (3)]. However, the monitored data of the deposition rate decrease. This behavior cannot be explained by a diffusion model [Eq. (3)]. In fact, the shear dispersion rather than the molecular diffusion mechanism dominate the wax deposition process. It is worth pointing out that the pipe flow would be "cold," and the wax crystals are suspended in the bulk flow for the above thermal condition, in which the oil temperature is held below the WAT. As explained previously, the precipitated waxes with lower carbon number are in the majority of the solution in the temperature range between 10 and 15 °C, and thus the yielded wax deposit tends to

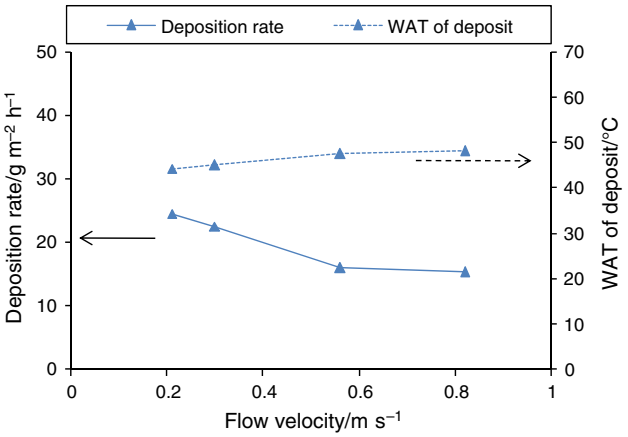

Fig. 10 Effect of oil flow velocity on the deposition characteristics under a specified thermal condition

contain much more waxes with lower carbon number. However, these lower carbon number waxes are easily stripped down by the flow shear due to the sloughing effect. As a result, a higher flow rate contributes to a lower wax deposition rate. Similar trends are also reported in previous studies [1, 27, 29, 31, 57, 77].

The radial temperature gradient in the vicinity of the pipe wall can be determined by a heat-transfer balance imposed at the wall [6]:

$$\left.\frac{\mathrm{d}T}{\mathrm{d}r}\right|_{\mathrm{w}} = \frac{Gc}{\lambda \pi d}\frac{\mathrm{d}T}{\mathrm{d}L}, \tag{5}$$

where $\left.\frac{\mathrm{d}T}{\mathrm{d}r}\right|_{\mathrm{w}}$ is the radial temperature gradient in the vicinity of the pipe wall in °C m^{-1}, G the mass flow rate in kg s^{-1}, c the specific heat of the crude oil in J kg^{-1} °C^{-1}, λ the heat conductivity for the crude oil in W m^{-1} °C^{-1}, d the inner diameter in m, and $\frac{\mathrm{d}T}{\mathrm{d}L}$ is the temperature drop per unit length in °C m^{-1}.

By introducing the new parameters *Pr* and *Re*, Eq. (5) becomes

$$\left.\frac{\mathrm{d}T}{\mathrm{d}r}\right|_{w} = \frac{1}{4} Pr \cdot Re \cdot \frac{\mathrm{d}T}{\mathrm{d}L}, \tag{6}$$

where *Pr* is the Prandtl number of the crude oil, $Pr = \frac{\mu c}{\lambda}$, in this relation μ is the viscosity of the crude oil in Pa s; *Re* is the Reynolds number of the crude oil, $Re = \frac{\rho v d}{\mu}$, ρ is the oil density in kg m^{-3}, and v is the oil flow velocity in m s^{-1}.

A cold-finger investigation for the wax deposition indicated that the predominant effect of the increasing shear stress is the removal of entrained oil [51]. In addition, Venkatesan [24] observed that the total deposition rate is decreased, and the wax content in the deposit is increased with the increasing shear under both the laminar and turbulent flow conditions. In order to further understand the influence of shear on the wax composition in the deposit,

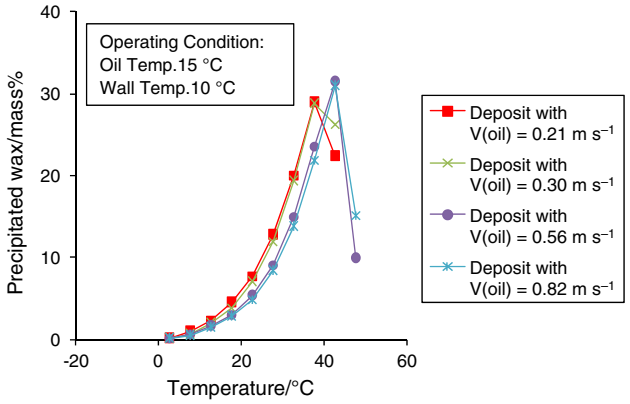

Fig. 11 Comparison of WPCs determined by DSC analysis for the flow loop wax deposits formed under different oil flow velocities with oil temperature of 15 °C and wall temperature of 10 °C

the deposit samples collected from the experiments described in this section were analyzed by DSC. Figure 10 shows the WAT of the deposit from various flow velocities. During the experiments, the oil and wall temperature were kept constant at 15 and 10 °C, respectively. The WAT of the deposit increases with the increasing flow velocity. This result not only agrees well with the result of Huang [69], but also confirms the conclusion reported by Jennings et al. [51] from the other viewpoint. For the increasing flow velocity, the adhesion of lighter hydrocarbons was so low that they may be stripped from the already deposited wax layer by the shear force; thus, the mass percentage of the heavier hydrocarbons in the deposit becomes relatively higher. As a result, a deposit with a higher WAT yields for a higher flow velocity.

Figure 11 shows a comparison of WPCs for the wax deposits that were retrieved from the above mentioned experiments. For every flow velocity investigated, the mass fraction of the crystallized waxes showed a maximum when plotted as a function of the cooling temperature. This peak value was higher at a higher flow velocity. This implies that much more waxes crystallized at the corresponding peak temperature for a higher flow velocity condition. Also, this maximum did not occur at the same value of the crystallized temperature for all the flow velocities studied. At a higher flow velocity, this maximum occurred at a higher temperature. Accordingly, the crystallization temperature domain shifted from the low temperature region toward the high temperature region. This shift to a higher crystallization temperature reflects the effect of operating flow velocity on wax composition in the deposit. However, the shift of wax composition in the deposit for varying flow velocities is slight, especially for the two adjacent WPCs. This is the result from the smaller changes for the flow velocities. When the flow velocity is varied significantly, the shift will be also much more evident. This result implies that the wax species finally deposited change toward a higher carbon number (a higher molecular mass distribution) for a higher operating flow velocity. Such behavior follows the trends of the WAT of the deposit shown in Fig. 10 for the same deposition tests. All these results imply a higher operating flow velocity that contributes to a wax deposit with heavier hydrocarbons. Also this conclusion verifies the experimental results regarding the wax content within the deposit by Singh et al. [21] and Hoffmann et al. [19].

Conclusions

A small-scale flow loop apparatus in combination with DSC technique has been used to investigate the wax deposition characteristics including the wax composition in deposit, and the influence of oil temperature, wall temperature, temperature difference between the bulk and the ambient, and the flow velocity were all studied in-depth. For a deposition experiment at a constant wall temperature, an increase in the oil temperature results in a higher deposition rate, whereas an increase in the wall temperature for a constant oil temperature leads to a lower deposition rate. A wax deposition peak may exist for a constant temperature difference condition. In addition, increasing flow velocity decreases the deposition rate.

The wax deposits retrieved from the flow loop were performed using DSC analysis after each deposition experiment. The examination of deposits by DSC with special designed method in this work clearly indicates that a wax deposit with heavier hydrocarbons was obtained when all the operating conditions evaluated were increased. Especially, the dependence of deposit characteristics on the operating oil temperature and temperature difference ΔT, which is poorly understood previously, was elucidated in the current work. This investigation for the effect of operating conditions on wax composition in the deposit will promote the understanding of the physic of the wax deposition. Moreover, it will provide a solid experimental basis for quantifying the mechanical hardness of the deposit, which is an important parameter for pipeline pigging.

Acknowledgements This work was supported by two grants from the National Natural Science Foundation of China (No. 51374224 and No. 51134006).

References

1. Singh P, Venkatesen R, Fogler HS, Nagarajan NR. Morphological evolution of thick wax deposits during aging. AIChE J. 2001;47:6–18.
2. Hammami A, Ratulowski J, Coutinho JAP. Cloud points: can we measure or model them? Pet Sci Technol. 2003;21:345–58.

3. Li HY, Zhang JJ. A generalized model for predicting non-Newtonian viscosity of waxy crudes as a function of temperature and precipitated wax. Fuel. 2003;82:1387–97.
4. Yan DF, Luo ZM. Rheological properties of Daqing crude oil and their application in pipeline transportation. SPE Prod Eng. 1987;2:267–76.
5. Bern PA, Withers VR, Cairns RJR. Wax deposition in crude pipelines. In: Proceedings of the European Offshore Petroleum Conference and Exhibition; London, UK, Oct 21–24, 1980; Paper EUR 206.
6. Burger ED, Perkins TK, Striegler JH. Studies of wax deposition in the Trans Alaska Pipeline. J Pet Technol. 1981;33:1075–86.
7. Weingarten JS, Euchner JA. Methods for predicting wax precipitation and deposition. SPE Prod Eng. 1988;2:121–6.
8. Hamouda AA, Viken BK. Wax deposition mechanism under high-pressure and in presence of light hydrocarbons. In: Proceedings of the SPE International Symposium on Oilfield Chemistry; New Oreleans, LA, 1993;SPE 25189.
9. Majeed A, Bringedal B, Overa S. Model calculates wax deposition for North Sea oil. Oil Gas J. 1990;18:52–9.
10. Brown TS, Niesen VG., Erickson DD. Measurement and prediction of the kinetics of paraffin deposition. In: Proceedings of the 68th Annual Technical Conference and Exhibition of the SPE; Houston, TX, Oct 3–6, 1993;SPE 26548.
11. Hsu JJC, Santamaria MM, Brubaker JP. Wax deposition of waxy live crudes under turbulent flow conditions. Proceedings of the 69th Annual Technical Conference and Exhibition of the SPE; New Orleans, LA, Sept 25–28, 1994;SPE 28480.
12. Matzain A. Single phase liquid paraffin deposition modeling. M.S. Thesis, University of Tulsa, Tulsa, OK, 1996.
13. Rygg OB, Rydahl AK, Ronningsen HP. Wax deposition in offshore pipeline systems. In: Proceedings of the 1st North American Conference on Multiphase Technology; Banff, Canada, June 10–11, 1998; BHR Group Limited: p. 193–203.
14. Creek JL, Matzain, A, Apte MS, Brill JP, Volk M., Delle Case E, Lund H. Mechanism for wax deposition. In: Proceedings of the 1999 AIChE Spring National Meeting; Houston, TX, Mar 15–18, 1999.
15. Matzain A, Apte MS, Zhang HQ, Volk M, Brill JP, Creek JL. Investigation of paraffin deposition during multiphase flow in pipelines and wellbores—part 1: experiments. ASME J Energ Resour Technol. 2002;124:180–6.
16. Apte MS, Matzain A, Zhang HQ, Volk M, Brill JP, Creek JL. Investigation of paraffin deposition during multiphase flow in pipelines and wellbores—part 2: modeling. ASME J Energ Resour Technol. 2001;123:150–7.
17. Azevedo LFA, Teixeira AM. A critical review of the modeling of wax deposition mechanisms. Pet Sci Technol. 2003;21:393–408.
18. Tinsley JF, Prud'homme RK, Guo XH, Adamson DH, Callahan S, Amin D, Shao SS, Kriegel RM, Saini R. Novel laboratory cell for fundamental studies of the effect of polymer additives on wax deposition from model crude oils. Energy Fuels. 2007;21:1301–8.
19. Hoffmann R, Amundsen L. Single-phase wax deposition experiments. Energy Fuels. 2010;24:1069–80.
20. Aiyejina A, Chakrabarti DP, Pilgrim A, Sastry MKS. Wax formation in oil pipelines: a critical review. Int J Multiph Flow. 2011;37:671–94.
21. Singh P, Venkatesan R, Fogler HS, Nagarajan NR. Formation and aging incipient thin film wax–oil gels. AIChE J. 2000;46:1059–73.
22. Solaimany Nazar AR, Dabir B, Islam MR. Experimental and mathematical modeling of wax deposition and propagation in pipes transporting crude oil. Energ. Source. 2005;27:185–207.
23. Correra S, Fasano A, Fusi L, Merino-Garcia D. Calculating deposit formation in the pipelining of waxy crude oils. Meccanica. 2007;42:149–65.
24. Venkatesen, R. The deposition and rheology of organic gels. Ph.D. Thesis, University of Michigan, Ann Arbor, MI, 2003.
25. Matzain, A. Multiphase flow paraffin deposition modeling. Ph.D. Thesis, University of Tulsa, Tulsa, OK, 1999.
26. Ribeiro FS, Mendes PRS, Braga SL. Obstruction of pipelines due to paraffin deposition during the flow of crude oils. Int J Heat Mass Transfer. 1997;18:40–8.
27. Bidmus HO, Mehrotra AK. Heat-transfer analogy for wax deposition from paraffinic mixtures. Ind Eng Chem Res. 2004;43:791–803.
28. Bhat NV, Mehrotra AK. Modeling of deposit formation from "waxy" mixtures via moving boundary formulation: radial heat transfer under static and laminar flow conditions. Ind Eng Chem Res. 2005;44:6948–62.
29. Parthasarathi P, Mehrotra AK. Solid deposition from multicomponent wax–solvent mixtures in a benchscale flow-loop apparatus with heat transfer. Energy Fuels. 2005;19:1387–98.
30. Mehrotra AK, Bhat NV. Modeling the effect of shear stress on deposition from "waxy" mixtures under laminar flow with heat transfer. Energy Fuels. 2007;21:1277–86.
31. Fong N, Mehrotra AK. Deposition under turbulent flow of wax–solvent mixtures in a bench-scale flow-loop apparatus with heat transfer. Energy Fuels. 2007;21:1263–76.
32. Bidmus HO, Mehrotra AK. Measurement of the liquid-deposit interface temperature during solids deposition from wax–solvent mixtures under static cooling conditions. Energy Fuels. 2008;22:1174–82.
33. Bidmus HO, Mehrotra AK. Solids deposition during "cold flow" of wax–solvent mixtures in a flow-loop apparatus with heat-transfer. Energy Fuels. 2009;23:3184–94.
34. Bidmus HO, Mehrotra AK. Measurement of the liquid-deposit interface temperature during solids deposition from wax–solvent mixtures under sheared cooling. Energy Fuels. 2008;22:4039–48.
35. Bhat NV, Mehrotra AK. Modeling the effect of shear stress on the composition and growth of the deposit layer from 'waxy' mixtures under laminar flow in a pipeline. Energy Fuels. 2008;22:3237–48.
36. Mehrotra AK, Bhat NV. Deposition from 'waxy' mixtures under turbulent flow in pipelines: inclusion of a viscoplastic deformation model for deposit aging. Energy Fuels. 2010;24:2240–8.
37. Fasano A, Fusi L, Correra S. Mathematical models for waxy crude oils. Meccanica. 2004;39:441–82.
38. Hamouda AA, Ravnoy JM. Prediction of wax deposition in pipelines and field experience on the influence of wax on drag-reducer performance. In: Proceedings of the 24th Annual Offshore Technology Conference; Houston, TX, 1992; OTC 7060.
39. Hsu JJC, Brubaker JP. Wax deposition scale-up modeling for waxy crude production lines. In: Proceedings of the 27th Annual Offshore Technology Conference; Houston, TX, May 1-4, 1995; OTC 7778.
40. Hsu JJC, Lian SJ, Liu M, Bi, HX, Guo CZ. Validation of wax deposition model by a field test. In: Proceedings of the SPE International Conference and Exhibition, Beijing, China, 1998;SPE 48867.
41. Lund HJ. Investigation of paraffin deposition during single-phase liquid flow in pipelines. M.S. Thesis, University of Tulsa, Tulsa, OK, 1998.
42. Hernandez OC. Investigation of single-phase paraffin deposition characteristics. M.S. Thesis, University of Tulsa, Tulsa, OK, 2002.
43. Hernandez OC, Hensly H, Sarica C. Improvements in single-phase paraffin deposition modeling. SPE Prod Facil. 2004;11:237–44.
44. dos Santos JST, Fernandes AC, Giulietti M. Study of the paraffin deposit formation using the cold finger methodology for Brazilian crude oils. J Pet Sci Eng. 2004;45:47–60.

45. Merino-Garcia D, Margarone M, Correra S. Kinetics of waxy gel formation from batch experiments. Energy Fuels. 2007;21:1287–95.
46. Zougari M, Sopkow T. Introduction to crude oil wax crystallization kinetics: process modeling. Ind Eng Chem Res. 2007;46:1360–8.
47. Huang QY. Modeling of wax deposition on waxy crude pipelines. Ph.D. Thesis, China University of Petroleum, Beijing, 2000.
48. Huang QY, Li YX, Zhang JJ. Unified wax deposition model. Acta Petrolei Sinica. 2008;29(3):459–62.
49. Correra S, Fasano A, Fusi L, Primicerio M. Modeling wax diffusion in crude oils: the cold finger device. Appl Math Modell. 2007;31:2286–98.
50. Venkatesan R, Creek JL. Wax deposition during production operations: SOTA. In: Proceedings of the 2007 Offshore Technology Conference; Houston, TX, 2007; OTC 18798.
51. Jennings DW, Weispfenning K. Effects of shear and temperature on wax deposition: coldfinger investigation with a Gulf of Mexico crude oil. Energy Fuels. 2005;19:1376–86.
52. Venkatesan R, Nagarajan NR, Paso K, Yi YB. The strength of paraffin gels formed under static and flow conditions. Chem Eng Sci. 2005;60:3587–98.
53. Huang ZY, Lu YD, Hoffmann R, Amundsen L, Fogler HS. The effect of operating temperatures on wax deposition. Energy Fuels. 2011;25:5180–8.
54. Bidmus HO, Mehrotra AK. Comments on "The effect of operating temperatures on wax deposition" by Huang et al. Energy Fuels. 2012;26:3963–6.
55. Merino-Garcia D, Correra S. Cold flow: a review of a technology to avoid wax deposition. Pet Sci Technol. 2008;26:446–59.
56. Valinejad R, Solaimany Nazar AR. An experimental design approach for investigating the effects of operating factors on the wax deposition in pipelines. Fuel. 2013;106:843–50.
57. Tiwary R, Mehrotra AK. Deposition from wax–solvent mixtures under turbulent flow: effects of shear rate and time on deposit properties. Energy Fuels. 2009;23:1299–310.
58. Alcázar-Vara LA, Buenrostro-Gonzalez E. Characterization of the wax precipitation in Mexican crude oils. Fuel Process Technol. 2011;92:2366–74.
59. Rønningsen HP, Bjørndal B, Hansen AB, Pedersen WB. Wax precipitation from North Sea oils: 1. Crystallization and dissolution temperature and Newtonian and non-Newtonian flow properties. Energy Fuels. 1991;5:895–908.
60. Alcazar-Vara LA, Buenrostro-Gonzalez E. Experimental study of the influence of solvent and asphaltenes on liquid–solid phase behavior of paraffinic model systems by using DSC and FT-IR techniques. J Therm Anal Calorim. 2012;107(3):1321–9.
61. Vieira LC, Buchuid MB, Lucas EF. Evaluation of pressure on the crystallization of waxes using microcalorimetry. J Therm Anal Calorim. 2013;111(1):583–8.
62. Kök MV, Letoffe JM, Claudy P. DSC and rheometry investigations of crude oils. J Therm Anal Calorim. 1999;56:959–65.
63. Kök MV, Letoffe JM, Claudy P. Comparative methods in the determination of wax content and pour points of crude oils. J Therm Anal Calorim. 2007;90(3):827–31.
64. Zhao YS, Paso K, Sjöblom J. Thermal behavior and solid fraction dependent gel strength model of waxy oils. J Therm Anal Calorim. 2014;. doi:10.1007/s10973-014-3660-3.
65. Mothé MG, Mothé CG, de Carvalho CHM, de Oliveira MCK. Thermal investigation of heavy crude oil by simultaneous TG–DSC–FTIR and EDXRF. J Therm Anal Calorim. 2013;113(2):525–31.
66. Díaz-Ponce JA, Flores EA, Lopez-Ortega A, Hernández-Cortez JG, Estrada A, Castro LV, Vazquez F. Differential scanning calorimetry characterization of water-in-oil emulsions from Mexican crude oils. J Therm Anal Calorim. 2010;102(3):899–906.
67. Han SP, Huang ZY, Senra M, Hoffmann R, Fogler HS. Method to determine the wax solubility curve in crude oil from centrifugation and high temperature gas chromatography measurements. Energy Fuels. 2010;24:1753–61.
68. Coto B, Martos C, Espada JJ, Robustillo MD, Merino-Garcia D, Pena JL. A new DSC-Based method to determine the wax porosity of mixtures precipitated from crude oils. Energy Fuels. 2011;25:1707–13.
69. Huang QY, Wang JF, Zhang JJ. Physical properties of wax deposits on the walls of crude pipelines. Pet Sci. 2009;6:64–8.
70. Li HY, Huang QY, Zhang F, Zhang JJ. Determination of wax content in crude oil using differential scanning calorimetry. J Univ Petrol China. 2003;27(1):60–2.
71. Gong J, Zhang Y, Liao LL, Duan JM, Wang PY, Zhou J. Wax deposition in the oil/gas two-phase flow for a horizontal pipe. Energy Fuels. 2011;25:1624–32.
72. Lashkarbolooki M, Seyfaee A, Esmaeilzadeh F, Mowla D. Experimental investigation of wax deposition in Kermanshah crude oil through a monitored flow loop apparatus. Energy Fuels. 2010;24:1234–41.
73. Chen XT, Butler T, Brill JP. Techniques for measuring wax thickness during single and multiphase flow. In: Proceedings of the 1997 SPE Annual Technical Conference and Exhibition; San Antonio, TX, Oct 5–8, 1997;SPE 38773.
74. Chakrabarti DP, Das G, Das PK. The transition from water continuous to continuous flow pattern. AIChE J. 2006;52:3668–78.
75. Zhang JJ, Liu ZH, Zhang F, Huang QY, Yan DF. Waxy crude treated with pour-point-depressants: flow behaviour and its evaluation. In: Proceedings of the 1997 International Symposium on Mutiphase, Non-Newtonian and Reacting Flows (ISMNRF); Beijing, P. R. China, Oct 7–10, 1997; International Academic Press: 7-15–7-20.
76. Wardhaugh LT, Boger DV. Flow characteristics of waxy crude oils: application to pipeline design. AIChE J. 1991;37:871–85.
77. Creek JL, Lund HJ, Brill JP, Volk M. Wax deposition in single phase flow. Fluid Phase Equilib. 1999;158:801–11.